Journal of Civil Engineering and Architecture 20 (2026) 376-384
doi: 10.17265/1934-7359/2026.09.002

Seismic Vulnerability Assessment of Heritage Masonry Building Bal Mandir

Pushp Raj Poudel[1] and Gokarna Bahadur Motra[2]

1. Department of Civil Engineering, Thapathali Campus, IOE, TU, Kathmandu 44600, Nepal

2. Department of Civil Engineering, IOE, TU, Lalitpur 44700, Nepal

Abstract: Heritage masonry buildings in Kathmandu Valley are highly vulnerable to earthquake damage because of their age, unreinforced masonry construction, weak mortar, irregular geometry, and limited seismic detailing. This study evaluates the seismic vulnerability of Bal Mandir, a historic Rana-era masonry building in Kathmandu, Nepal, using a 3 Dimensional macro finite element model (FEM) developed in ETABS v20. Material properties were obtained from relevant literature, and seismic loading was defined in accordance with NBC 105:2020. The building was analyzed using response spectrum analysis and linear time-history analysis with seven earthquake ground-motion records matched to the target response spectrum. The first-mode period obtained from the numerical model was 0.348 s, which was close to the empirical value recommended by NBC 105:2020. Fragility curves were developed using roof-displacement demand obtained from the time-history analyses and damage-state thresholds adopted from the FEMA HAZUS-MH methodology for the URMM (Unreinforced Masonry, Mid-Rise) building class. At the Kathmandu design PGA of 0.35 g, corresponding to a 475-year return period, the probabilities of exceedance for Slight, Moderate, Extensive, and Complete damage were estimated as 100%, 99.32%, 84.03%, and 55.17%, respectively. The results indicate a high likelihood of severe damage under the design-level earthquake and highlight the need for appropriate seismic strengthening and conservation measures for Bal Mandir. The assessment is based on linear structural analysis and generalized HAZUS damage thresholds and should therefore be interpreted as a global vulnerability estimate rather than a detailed prediction of local nonlinear damage mechanisms.

Keywords: Seismic Vulnerability assessment; Fragility curve; Macro modelling; Linear time-history analysis; HAZUS-MH; ETABS.

1. Introduction

Nepal lies in a highly seismically active region, where past earthquakes have caused significant casualties, infrastructure damage, and economic losses [1]. The Kathmandu Valley also contains many historic cultural assets, including Hindu temples, Buddhist monasteries, and Rana-era palaces. Many of these structures were built using traditional masonry systems with mud mortar, lime-surkhi mortar, and locally available materials, giving the Valley its peculiar architectural and cultural character [2].

Historic masonry buildings are particularly vulnerable to earthquakes because of aging materials, weak connections, limited lateral-load resistance, and inadequate seismic detailing. Severe ground shaking can therefore lead to substantial structural damage or collapse. Previous observations have shown that deficiencies in the structural system and limited post-disaster intervention can further increase the vulnerability of heritage buildings [3]. A reliable understanding of their seismic behavior is therefore essential for identifying weaknesses and developing appropriate strengthening and conservation measures [3].

Seismic vulnerability assessment provides a quantitative basis for evaluating expected damage under different levels of earthquake intensity. Fragility curves are commonly used for this purpose because they make the

Corresponding author: Pushp Raj Poudel, M.Sc. Earthquake Engineering, M.E. Civil Engineering, Ph.D. student; Research fields: structural/earthquake engineering, structural control and dynamics, seismic vulnerability assessment, and finite element analysis.

relationship of intensity of seismic event to the probability of exceeding predefined damage states. Such relationships can support performance evaluation, retrofitting decisions, and conservation planning, while allowing traditional materials such as brick masonry, lime-surkhi mortar, and mud mortar to be considered together with compatible strengthening techniques [4].

In this study, Bal Mandir, also known as Tangal Durbar or Sita Mahal, was selected as a representative Rana-era heritage masonry building in Kathmandu. The building is currently occupied by the Nepal Children's Organization (NCO) and the Nepal Academy of Fine Arts (NAFA) . The objective of this study is to evaluate its seismic vulnerability by developing fragility curves for different structural damage states under varying levels of earthquake ground motion.

2. Objective

The objective of this study is to assess the seismic vulnerability of Bal Mandir by developing fragility curves from linear time-history analysis and estimating the probability of exceeding different structural damage states under varying levels of earthquake ground motion.

3. Methodology

3.1 Building Description

Bal Mandir is believed to have been constructed around 1988/89 Bikram Sambat (B.S.), based on inscriptions on brick units reading "Shree Tin Bhim 1988" and "Shree Tin Bhim 1989." Bhim Shumsher Jung Bahadur Rana, then Prime Minister of Nepal, named the palace "Sita Palace" after his wife and later transferred it to his third son, Ram Shumsher. Following Ram Shumsher's death, the property was sold to the Government of Nepal.

The building is predominantly constructed of unreinforced brick masonry in mud mortar, with lime-surkhi mortar used locally in brick arches, circular columns, lintel zones, and beam-support regions. It is founded on stepped masonry footings and contains two courtyards. The ground-floor plinth area is approximately 2,627 m², with a total floor area of about 8,722 m². The overall plan dimensions are approximately 78.985 m in the east-west direction and 74.725 m in the north-south direction, excluding local extensions and projections. The front and rear courtyards measure approximately 30 m × 20 m and 24 m × 21 m, respectively. Interconnected brick-arch tunnels are present at ground-floor level for ventilation.

The first- and second-floor systems include brick jack arches supported by Indian Standard Medium Beams (ISMB) and Indian Standard Medium Channels (ISMC), over which lime concrete and floor finishes are placed. Timber floors consist of Sal wood joists of 100 × 125 mm at 300 mm center-to-center spacing, supported by 150 × 300 mm Sal wood beams spaced at approximately 1.8 m. Wall thickness varies by level, with typical values of 900 mm at the ground floor, 800 mm at the first and second floors, and 600–700 mm at the third-floor penthouse level. The parapet wall is approximately 225 mm thick and 900 mm high.

The roof is primarily supported by timber trusses spaced at about 2 m, with 100 × 125 mm common rafters at 550 mm center-to-center and 25 × 50 mm wooden battens at 350 mm center-to-center. Clay roof tiles are approximately 200 × 400 × 40 mm. The eastern wing contains a reinforced masonry sloping roof slab. The total building height is approximately 14.2 m, with varying story heights.

3.2 Material Properties

The material properties used for development of finite element model are presented in Table 1. Because detailed in-situ mechanical testing was not available for all constituent materials, representative properties were selected from relevant literature and previous studies on similar construction materials. The model includes masonry in mud mortar, masonry in lime-surkhi mortar, reinforced concrete, compacted mud flooring, and Sal wood. Young's modulus, Poisson's ratio, and unit weight were assigned as the primary elastic material parameters used in the analysis.

3.3 Numerical Modelling

A three-dimensional FE macro model of Bal Mandir was developed in ETABS v20 to represent the global structural response of the building. In the macro-modelling approach, the masonry walls were represented as equivalent continuum shell elements using the average mechanical properties assigned to the corresponding masonry type. The walls, which vary approximately from 600 to 900 mm in thickness, were modeled using two-dimensional shell elements. For computational simplicity, a uniform representative wall thickness was assigned at each story level while preserving the overall geometry and load-transfer system of the building.

The existing floor systems consist of brick jack arches and timber floors supported by steel or timber beams. Rather than modeling these components individually, the distributed dead load of the floor assembly, including floor finishes, was calculated and represented using equivalent reinforced-concrete slab elements spanning between the supporting walls. The principal timber and steel beams were modeled at their corresponding structural locations to maintain the primary gravity-load transfer mechanism. This idealization was adopted to reproduce the global mass distribution and load path while avoiding unnecessary geometric complexity.

The timber roof was not modeled explicitly as part of the lateral-load-resisting system. Instead, its gravity load was calculated and applied as distributed loading to the supporting masonry walls, reflecting the approximately uniform load transfer from the roof rafters. Live loads were assigned according to IS 875 (Part 2):1987 for institutional occupancy, with values of 3.0 kN/m^2 for rooms, 4.0 kN/m^2 for halls and corridors, 1.5 kN/m^2 for attics and terraces, and 0.75 kN/m^2 for tiled roofs. The resulting three-dimensional macro model is shown in Fig. 1.

3.4 Basic Response Spectrum

The seismic demand for the building was defined in accordance with NBC 105-2020 using the design acceleration response spectrum for Kathmandu. The site was assigned a seismic zone factor of $Z = 0.35$, corresponding to a 475-year return period, as specified in Table 4-5 of NBC 105-2020. An importance factor of $I = 1.25$ was adopted from Table 4-6. For the Kathmandu Valley, Soil Type D was selected in accordance with Section 4.1.3.4 and Table 4-4 of NBC 105:2020.

Using these parameters, the horizontal design spectrum was established for structural analysis. The resulting horizontal base-shear coefficient was calculated as 0.391, and the exponent related to the structural period was taken as 1. The response spectrum used in the analysis is shown in Fig. 2.

3.5 Linear Time History Analysis

For linear time-history analysis earthquake ground-motion data were downloaded for seven different earthquakes from the Pacific Earthquake Engineering Research Center (PEER) Ground Motion Database. The selected data were matched to the target response spectrum defined according to NBC 105-2020. The records were chosen to provide variation in earthquake magnitude, peak ground acceleration, duration, and frequency content so that the structural response could be evaluated under a range of ground-motion characteristics.

Table 1 Material properties used in the finite element model.

SN	Material	Young's modulus of elasticity, MPa	Poisson ratio	Unit Weight, kN/m^3	Source
1	Masonry in mud mortar	542	0.25	19.6	[3]
2	Masonry in lime surkhi mortar	1,358	0.25	19.6	[3]
3	Reinforced concrete(M15)	19,365	0.20	25.0	[3]
4	Compacted mud floor	30	0.30	18.0	[3]
5	Sal wood	12,500	0.35	8.65	[5, 6]

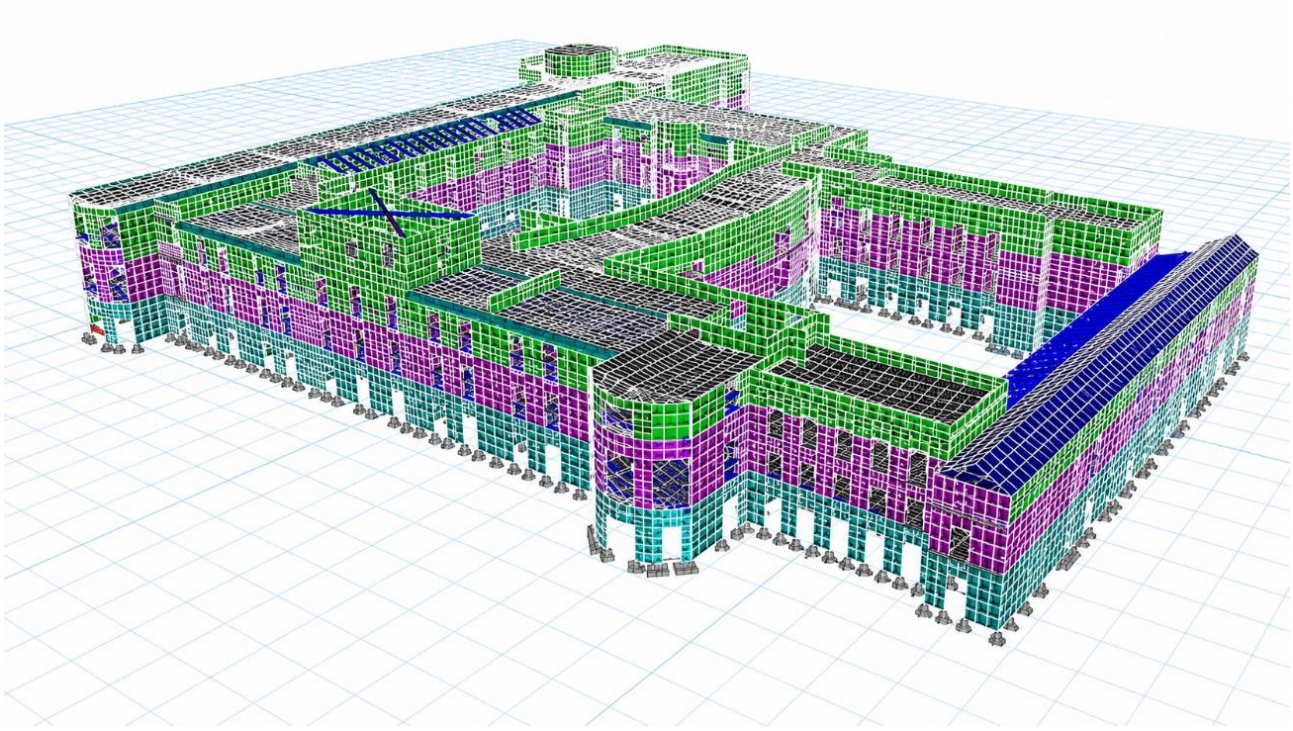


Fig. 1 3D macro element model in E-tabs V20.

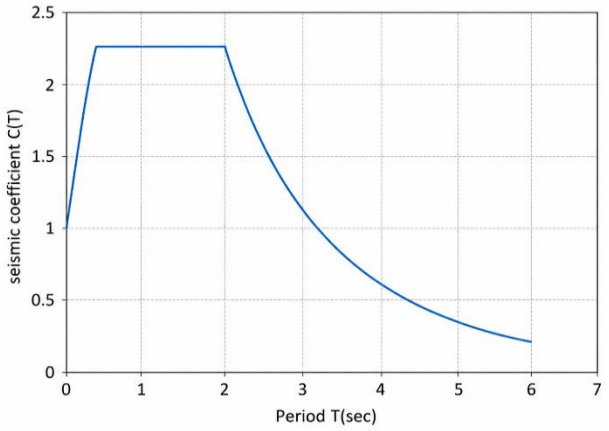


Fig. 2 Design response spectrum adopted from NBC 105:2020 for Soil Type D.

The selected earthquakes include the 2015 Gorkha, 1995 Kobe, 1952 Kern County, 1994 Northridge-01, 1989 Loma Prieta, 1999 Chi-Chi Taiwan, and 1940 Imperial Valley events. Their corresponding magnitudes, recording stations, and peak ground accelerations are summarized in Table 2. Representative accelerograms of the seven records are presented in Figs. 3–9.

The matched ground motions were applied to the numerical model to obtain the dynamic response of the building, including roof displacement and other global response quantities used in the subsequent fragility assessment.

3.6 Development of Fragility Curves

Vulnerability associated with seismic ground motion can be quantified using damage probability matrices or fragility curves [7]. In this study, seismic fragility was evaluated in terms of the probability that the structural demand exceeds predefined damage-state thresholds. A lognormal distribution was adopted to represent the probability of exceeding a damage state, ds, for a given spectral displacement demand, Sd, as [8].

$$P(ds \mid Sd) = \Phi\,[(1 / \beta ds)\, \ln (Sd / \bar{S}d,ds)] \qquad (1)$$

where, $\bar{S}d,ds$ is the median spectral displacement corresponding to the threshold of damage, ds, and βds is the logarithmic standard deviation representing uncertainty in the fragility relationship. A value of $\beta ds = 0.64$ was adopted for the unreinforced masonry building class considered in this study [8].

The four structural damage states-Slight, Moderate, Extensive, and Complete-were defined using the

FEMA HAZUS-MH methodology [8]. Bal Mandir was represented using the Unreinforced Masonry, Mid-Rise (URMM) building class as the closest available HAZUS classification for the heritage masonry system considered in this study. The corresponding damage-state displacement thresholds were defined as:

1. Slight damage state, capacity $\bar{S}d$, $S = 0.7 \times dy$,
2. Moderate damage, capacity $\bar{S}d$, $M = 1.5 \times dy$,
3. Extensive damage, capacity $\bar{S}d$, $E = 0.5 \times (dy + du)$,
4. Complete damage, capacity $\bar{S}d$, $C = du$.

where dy and du denote the yield and ultimate displacements, respectively. For the selected URMM building class, dy = 0.27 in. (6.858 mm) and du = 1.81 in. (45.974 mm) were adopted from the FEMA HAZUS-MH MR3 Technical Manual [8].

Table 2 Selected earthquake ground-motion records used in the linear time-history analysis.

S.N.	Description of earthquake	Magnitude (Mw)	Station	PGA (g)
1	Gorkha Earthquake (2015)	7.8	Kanti Path	0.164
2	Kobe Earthquake (1995)	6.9	Nishi-Akashi	0.483
3	Kern County Earthquake (1952)	7.36	Pasadena-CIT Athenaeum	0.053
4	Northridge-01 Earthquake (1994)	6.69	Anacapa Island	0.067
5	Loma Prieta Earthquake (1989)	6.93	Los Gatos-Lexington Dam	0.443
6	Chi-Chi Taiwan Earthquake (1999)	7.62	HWA002	0.091
7	Imperial Valley Earthquake (1940)	6.95	El Centro Array 9	0.281

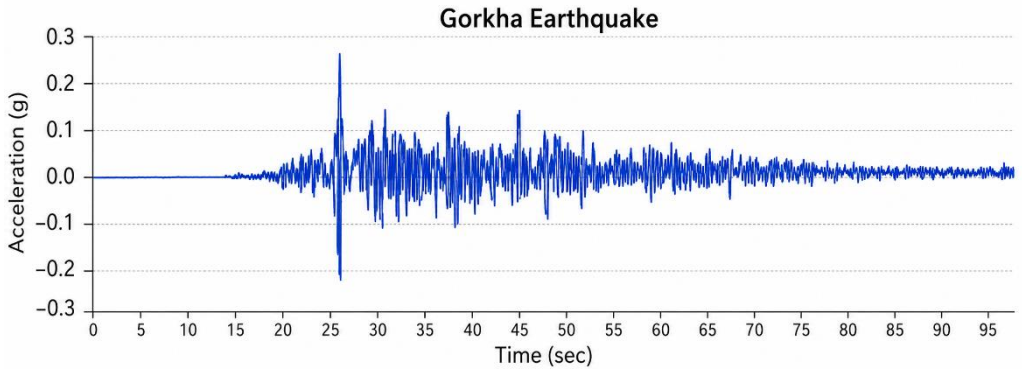


Fig. 3 Accelerogram of Gorkha Earthquake.

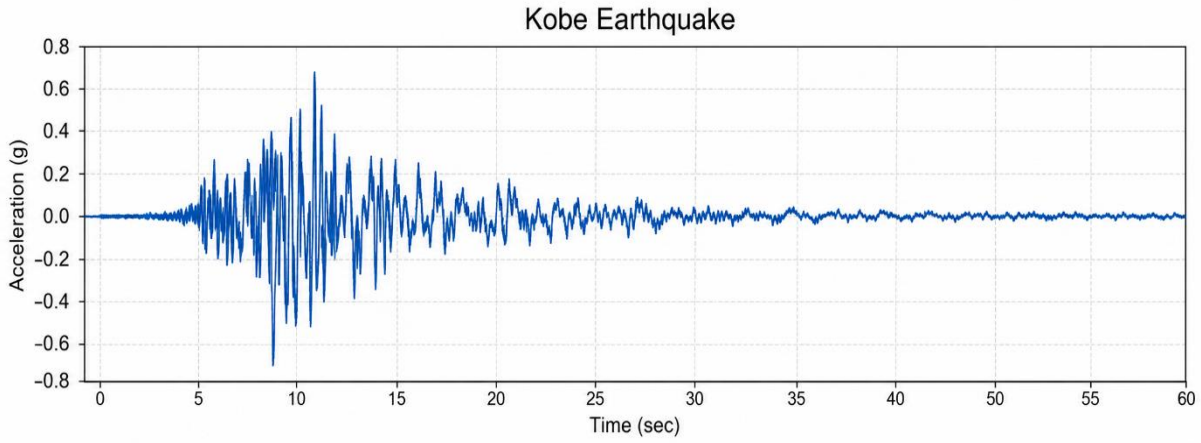


Fig. 4 Accelerogram of Kobe Earthquake.

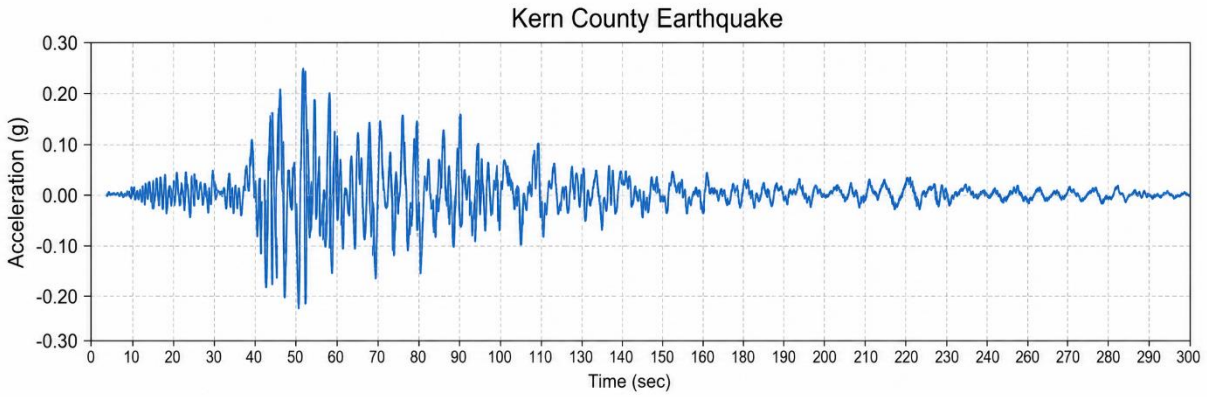


Fig. 5 Accelerogram of Kern County Earthquake.

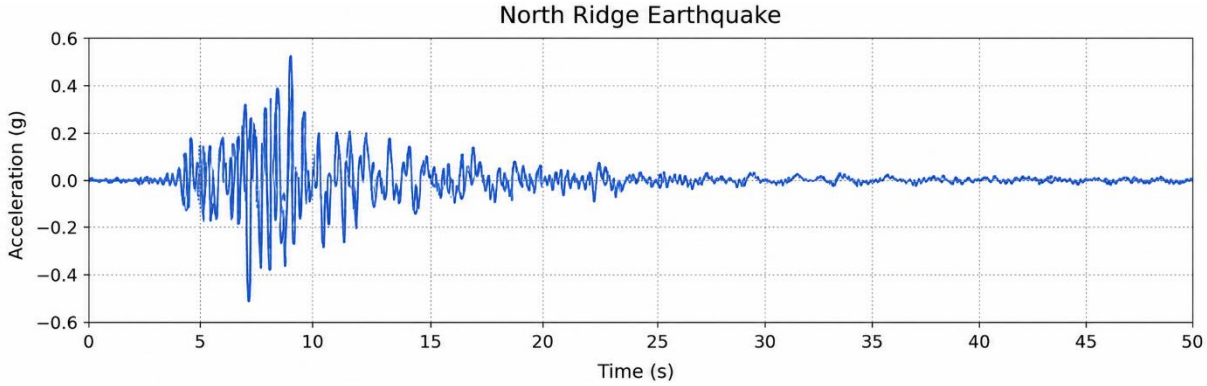


Fig. 6 Accelerogram of Northridge-01 Earthquake.

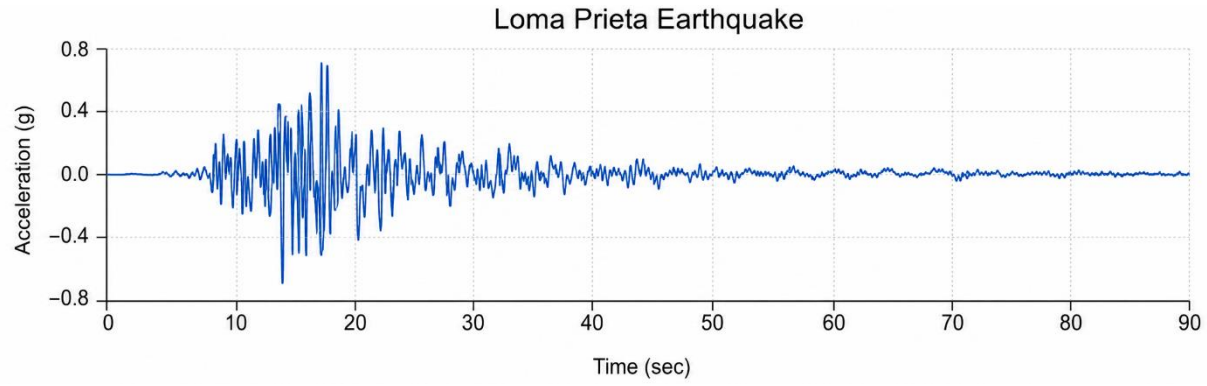


Fig. 7 Accelerogram of Loma Prieta Earthquake.

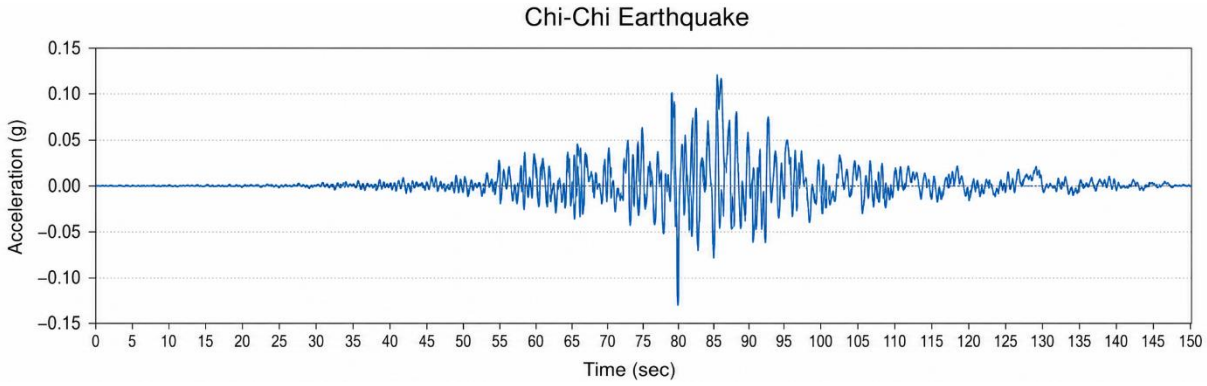


Fig. 8 Accelerogram of Chi-Chi Taiwan Earthquake.

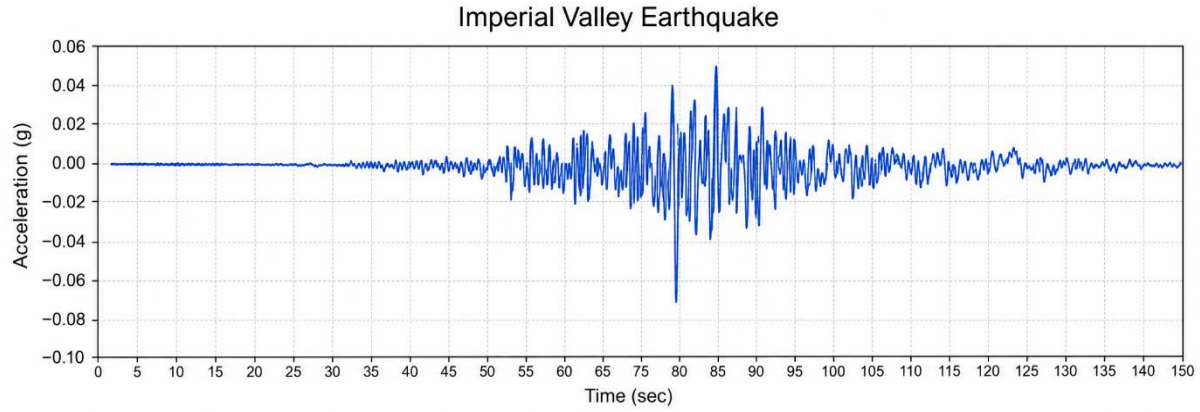


Fig. 9 Accelerogram of Imperial Valley Earthquake.

Table 3 Global model results.

S.N.	Parameters	X direction	Y direction
1	Base Shear (kN)	85,083.67	85,083.67

The maximum roof-displacement responses obtained from the seven linear time-history analyses were evaluated for PGA levels ranging from 0.1 g to 1.0 g and converted to spectral displacement demand. Linear regression was then used to establish the relationship between PGA and spectral displacement. This demand relationship, together with the HAZUS-based damage-state thresholds, was used to construct the fragility curves and estimate the probability of exceeding each damage state.

4. Results and Discussion

4.1 Global Structural Response

The three-dimensional ETABS model was analyzed to evaluate the global seismic response of Bal Mandir. The fundamental period obtained from the numerical model was 0.348 s. This value is reasonably close to the unamplified empirical period of 0.366 s estimated according to NBC 105-2020 for a building height of 14.2 m, providing a basic consistency check on the overall stiffness representation of the numerical model.

The design base shear obtained from the analysis was 85,083.67 kN in both the X and Y directions, as summarized in Table 3 above. The comparable values in the two principal directions reflect the seismic load definition adopted for the global analysis. These model results were subsequently used together with the linear time-history responses to evaluate the seismic demand and develop the fragility relationships for the building.

4.2 Capacity of Building Recommended by HAZUS (Hazard United States)

The damage-state displacement thresholds used in the fragility assessment were calculated from the HAZUS URMM (Unreinforced Masonry-based relationships defined in Section 3.6. Using the adopted yield displacement, dy = 6.858 mm, and ultimate displacement, du = 45.974 mm, the corresponding thresholds were obtained as follows:

1. Slight damage, capacity = 0.7dy = 0.7×6.858 = 4.801 mm.
2. Moderate damage, capacity = 1.5dy = 1.5×6.858 = 10.287 mm.
3. Extensive damage, capacity = 0.5 (dy + du) = 0.5 × (6.858+45.974) = 26.416 mm.
4. Complete damage, capacity = du = 45.974 mm.

4.3 Fragility Curve

Linear time-history analyses were carried out using the seven selected earthquake records, and the corresponding maximum roof-displacement responses were evaluated over PGA levels ranging from 0.1 g to 1.0 g. The resulting displacement demands were

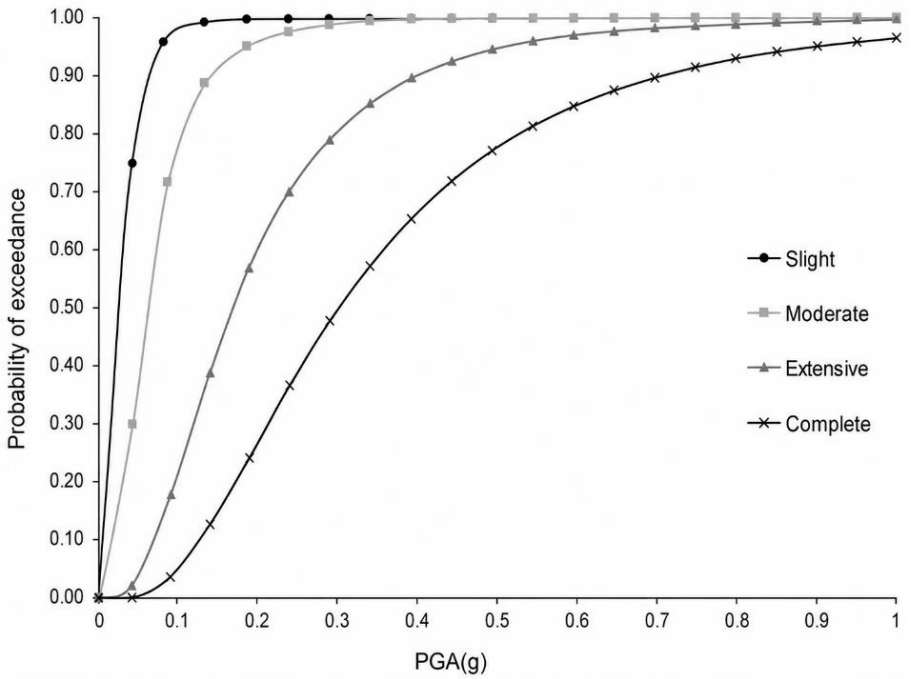


Fig. 10 Fragility curves for Bal Mandir showing the probability of exceedance of the four structural damage states.

converted to spectral displacement and used to establish the following linear regression relationship between spectral displacement and PGA:

$$Sd = 142.75 \times (PGA) \quad (2)$$

This relationship was combined with the damage-state thresholds defined in Section 4.2 and the lognormal fragility formulation presented in Section 3.6 to estimate the probability of exceeding each damage state.

At the Kathmandu design PGA of 0.35 g, corresponding to a 475-year return period according to NBC 105:2020, the probabilities of exceeding the Slight, Moderate, Extensive, and Complete damage states were estimated as 100%, 99.32%, 84.03%, and 55.17%, respectively. These results indicate that the building has a high probability of experiencing severe structural damage under the design-level earthquake, with an 84.03% probability of exceeding the Extensive damage state and a 55.17% probability of exceeding the Complete damage state. The resulting fragility curves are shown in Fig. 10.

5. Conclusion

A three-dimensional macro finite element model of Bal Mandir was developed in ETABS v20 to assess the global seismic vulnerability of the heritage masonry building. Seismic demand was evaluated using the NBC 105:2020 response spectrum and seven selected earthquake ground-motion records. The fundamental period obtained from the model was 0.348 s, which was reasonably close to the NBC 105:2020 empirical value of 0.366 s.

Fragility curves were developed from the linear time-history displacement demands using HAZUS-based URMM damage-state thresholds. The spectral displacement–PGA relationship was obtained as:

$$Sd = 142.75 \times PGA$$

At the Kathmandu design PGA of 0.35 g, the probabilities of exceeding the Slight, Moderate, Extensive, and Complete damage states were estimated as 100%, 99.32%, 84.03%, and 55.17%, respectively. These results indicate a high seismic vulnerability of Bal Mandir and suggest the need for appropriate strengthening and conservation measures. The developed fragility curves can support preliminary seismic risk assessment and intervention planning for similar heritage masonry buildings in Kathmandu Valley.

6. Limitations and Future Research

The present study is based on linear structural analysis and simplified macro-modelling assumptions; therefore, nonlinear masonry behavior, local failure mechanisms, and detailed material variability are not explicitly captured. In addition, HAZUS-based URMM damage thresholds were adopted as an approximate representation of the heritage masonry system.

Future studies should incorporate building-specific material testing, nonlinear static or time-history analysis, and uncertainty assessment to improve the accuracy of the fragility relationships and better represent the seismic behavior of Bal Mandir.

7. Data Availability Statement

The data used in this study will be available from the corresponding author upon reasonable request. Some building-related information and supporting data were obtained through site access and from Digicon Engineering Consult Pvt. Ltd.; therefore, public distribution of all source data may be subject to permission.

Acknowledgments

The authors would like to thank the Nepal Children's Organization for providing access to the building and Digicon Engineering Consult Pvt. Ltd. for providing relevant data. The authors also sincerely acknowledge Mr. Prashant Dhimal for his valuable assistance and support throughout the research work.

References

[1] Thapa, D. R. 2018. "Seismicity of Nepal and the Surrounding Region." *Bulletin of the Department of Geology* 20–21: 83–86. DOI: 10.3126/bdg.v20i0.20727.

[2] UNESCO World Heritage Centre. n.d. "Kathmandu Valley." https://whc.unesco.org/en/list/121

[3] Motra, G. B., Sah, B. K., and Jha, P. 2021. "Structural Condition Assessment and Retrofitting of Shital Niwas Building (Presidential Palace)." *Progress in Disaster Science* 10: 100174. DOI: 10.1016/j.pdisas.2021.100174.

[4] Government of Nepal, Department of Urban Development and Building Construction. 2017. *Seismic Retrofitting Guidelines of Buildings in Nepal: Compilation of Adobe, Masonry and RCC*. Kathmandu, Nepal. https://www.dudbc.gov.np/pages/building-code-section/

[5] Government of Nepal, Department of Urban Development and Building Construction. 1994. *Nepal National Building Code: Timber*. Kathmandu, Nepal. https://www.dudbc.gov.np/pages/building-code-section/

[6] Sonelastic®. n.d. "Modulus of Elasticity and Poisson's Coefficient of Wood." ATCP Physical Engineering. https://www.sonelastic.com/en/fundamentals/tables-of-materials-properties/woods

[7] Biglari, M., and Formisano, A. 2020. "Damage Probability Matrices and Empirical Fragility Curves from Damage Data on Masonry Buildings after Sarpol-e-Zahab and Bam Earthquakes of Iran." *Frontiers in Built Environment* 6: 2. DOI: 10.3389/fbuil.2020.00002.

[8] Federal Emergency Management Agency (FEMA). 2007. *HAZUS-MH MR3 Technical Manual: Earthquake Model*. Washington, DC: FEMA. https://www.fema.gov/sites/default/files/2020-09/fema_hazus_earthquake-model_technical-manual_2.1.pdf

[9] Government of Nepal, Department of Urban Development and Building Construction. 2020. *Nepal National Building Code NBC 105:2020: Seismic Design of Buildings in Nepal*. Kathmandu, Nepal. https://www.lsmcebps.gov.np/UploadFiles/NBC105_2020.pdf